Location effects of vanadium in NiFe layered double hydroxides for oxygen evolution reaction

Mengze Ma,[a] Yechi Zhang,[a] Xiaoqian Ding,[a] Jianlei Jing,[a] Linbo Jin,[a] Wei Liu,[a] Daojin Zhou*[a] and Xiaoming Sun*[a]

Supporting Information

Experimental Section

Chemicals: $Fe(NO_3)_3·9H_2O$, $Ni(NO_3)_2·6H_2O$, VCl_3, Na_2CO_3, $NaVO_3$, NaOH, KOH, deionized water, carbon paper, Ni foam, ethanol.

Synthesis of CO_3^{2-}-Ni_2Fe_1LDHs by co-precipitation method: $Ni(NO_3)_2·6H_2O$ (2 mmol) and $Fe(NO_3)_3·9H_2O$ (1 mmol) were dissolved in 30 mL deionized water named mixture aqueous A. Na_2CO_3 (0.6 g) and NaOH (0.6 g) were dissolved in 30 mL deionized water named mixture aqueous B. 30 mL was deionized water in beaker C. Dropping A and B simultaneously into C, maintaining aqueous pH at 10.0. Then keep stirring for 20min. The obtained turbid liquid was centrifuged 5 times with water washing every time. The obtained gelatinous precipitate placed in vacuum freeze dryer for 24h.

The VO_3^-- Ni_2Fe_1LDHs was synthesized by same method except for replacing $NaCO_3$ (0.6 g) with $NaCO_3$ (0.6 g) in aqueous B and bubbling N_2 in the whole reaction process.

Synthesis of $Ni_2Fe_xV_{(1-x)}$LDHs by co-precipitation method: $Ni(NO_3)_2·6H_2O$ (2 mmol), $Fe(NO_3)_3·9H_2O$ (x mmol) and VCl_3 [(1-x) mmol] (x = 0.1, 0.3, 0.5, 0.7, 0.9) were dissolved in 30 mL deionized water named mixture aqueous A. NaOH (0.6g) was dissolved in 30 mL deionized water named mixture aqueous B. 30 mL deionized water in beaker C. Dropping A and B simultaneously into C, maintaining aqueous pH at 10.0 with N_2 bubbling. Then keep stirring for 12h with N_2 bubbling. The obtained turbid liquid was centrifuged 5 times with water washing every time. The obtained gelatinous precipitate placed in vacuum freeze dryer for 24h.

The VO_3^-- $Ni_2Fe_{0.5}V_{0.5}$LDHs was synthesized by same method except for adding $NaVO_3$ (0.6 g) in aqueous B.

Electrochemical Measurements: In order to evaluate the OER performance of the as-prepared sample in alkaline electrolyte, a standard three-electrode glass cell connected to an electrochemical workstation (CHI 660E, CH, Shanghai.) was used for testing, in which the platinum electrode was used as the counter electrode and the Hg/HgO electrode was used as the reference electrode. The durable test was conducted in two electrode system connected with battery testing system (CT-4008-5V10A, NEWARE, Shenzhen). The preparation method of working electrode: 5 mg powder sample was dispersed homogeneously with 1 mL ethanol in centrifuge tube, than adding 20 μL 5% Nafion aqueous as binder named catalyst ink. Dropping ink at 1 cm×1 cm Ni foam slowly. Since the redox peak of Ni/Fe is former than OER, which will disturb the OER onset potential, so the reverse sweep of cyclic voltammetry is adopted.

When we characterized the catalyst after stability test with Ni foam as substate, it is difficult to get clear results due to the rough surface, so we replace Ni foam with carbon paper for the following test.

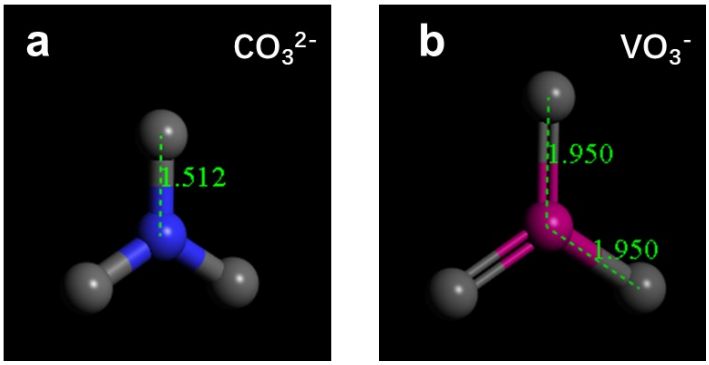

Figure S1. (a) and (b) Schematic diagram of anion structure of CO_3^{2-} and VO_3^-.

Table S1. Analytical results obtained by ICP-OES techniques of as-prepared CO_3^{2-}-Ni_2Fe_1LDHs and VO_3^-- Ni_2Fe_1LDHs.

	Element	**Mass fraction W（%）**
VO_3^--Ni_2Fe_1LDHs	Fe	15.030%
	Ni	29.850%
	V	9.812%
CO_3^{2-}-Ni_2Fe_1LDHs	Fe	17.787%
	Ni	35.385%
	V	<0.005

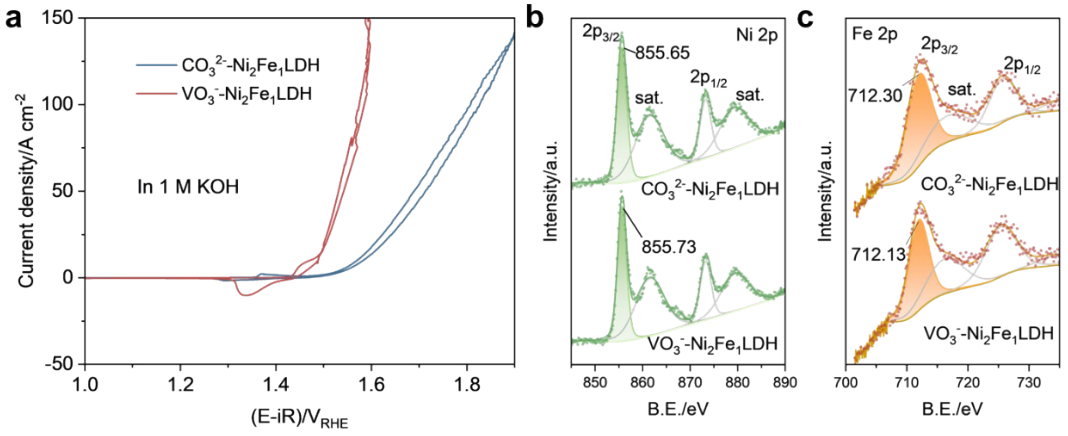

Figure S2. (a) Polarization curves of CO_3^{2-}-Ni_2Fe_1LDHs and VO_3^--Ni_2Fe_1LDHs tested in 1 M KOH, three electrode, XPS spectra of (b) Ni 2p and (c) Fe 2p and peak fitting analysis of CO_3^{2-}-Ni_2Fe_1LDHs and VO_3^--Ni_2Fe_1LDHs.

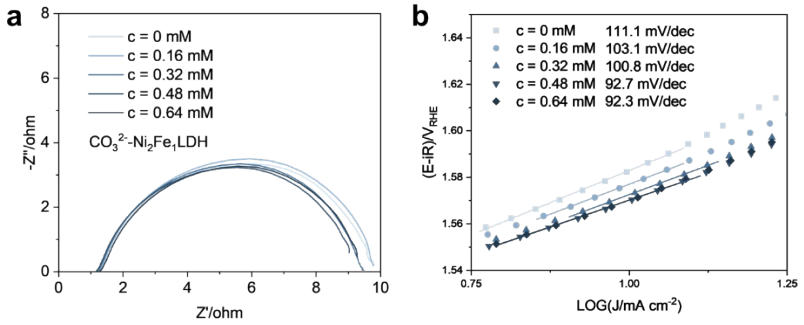

Figure S3. (a) and (b) EIS and Tafel slope of CO_3^{2-}-Ni_2Fe_1LDHs in 1 M KOH + c mM $NaVO_3$, respectively, EIS is tested at 0.6 $V_{Hg/HgO}$.

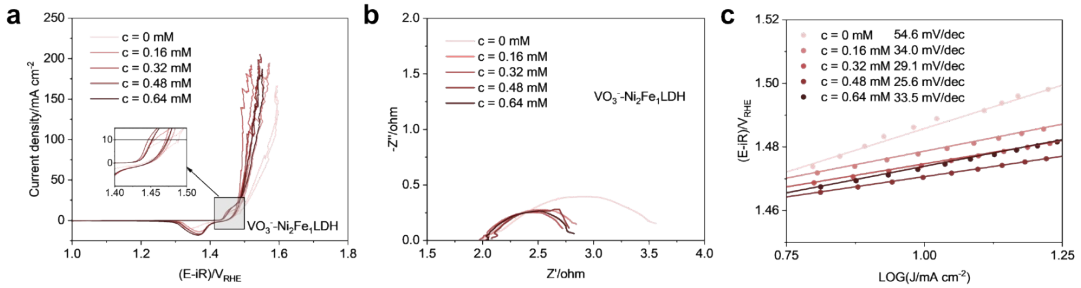

Figure S4. (a), (b) and (c) Cyclic Voltammetry, EIS and Tafel slope of VO_3^--NiFe LDHs in 1 M KOH + c mM $NaVO_3$, respectively, scan rate of CV is 5 mV/s, EIS is tested at 0.6 $V_{Hg/HgO}$.

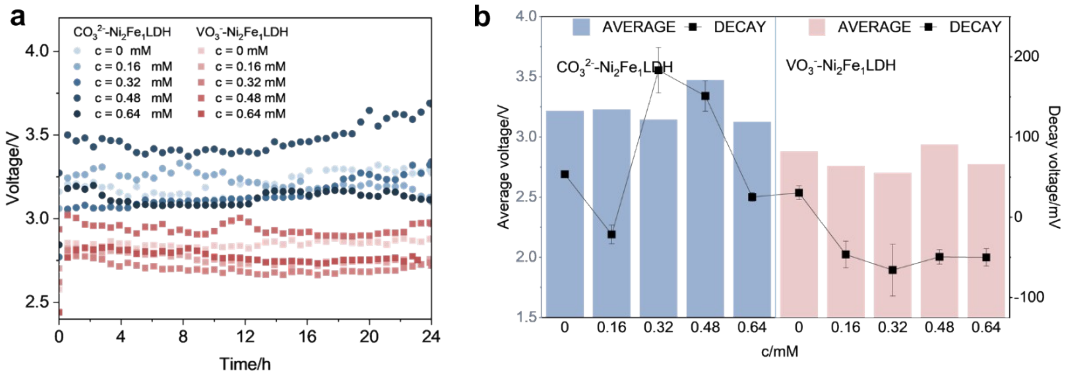

Figure S5. (a) Long-term stability data of CO_3^{2-}-Ni_2Fe_1LDHs and VO_3^--NiFe LDHs (400 mA/cm^2, 80℃, 24h) and (b) corresponding average voltage and decay voltage (with error bar tested 3 times, the same below).

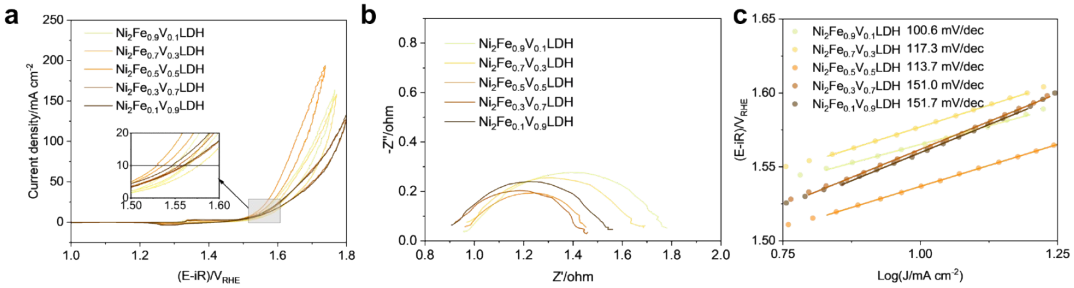

Figure S6. (a), (b) and (c) Cyclic Voltammetry, EIS and Tafel slope of $Ni_2Fe_xV_{(1-x)}$LDHs in 1 M KOH, respectively, scan rate of CV is 5 mV/s, EIS is tested at 0.6 $V_{Hg/HgO}$.

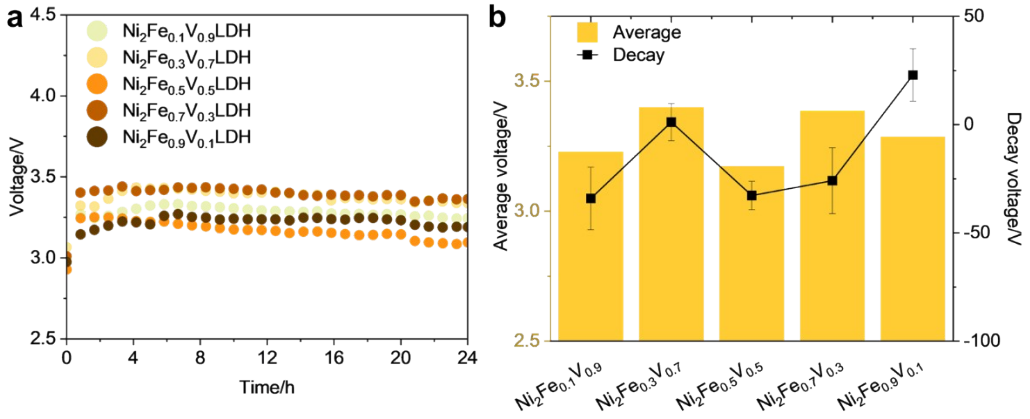

Figure S7. (a) Long-term stability curves of $Ni_2Fe_xV_{(1-x)}$LDHs (400 mA/cm^2, 80℃, 24h) and (b) corresponding average voltage and decay voltage.

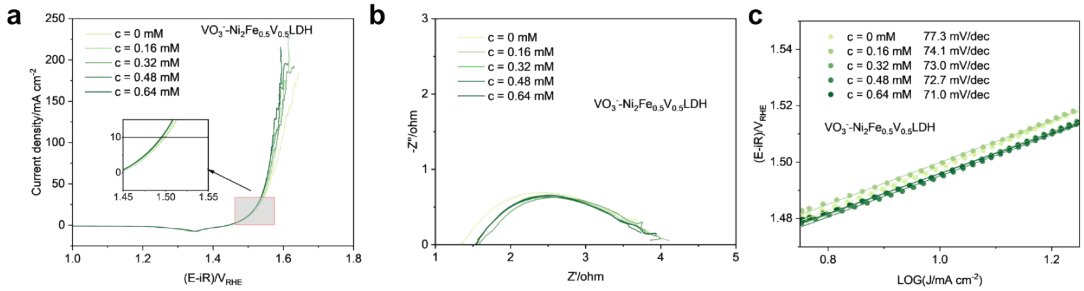

Figure S8. (a), (b) and (c) Cyclic Voltammetry (CV), EIS and Tafel slope of VO_3^--$Ni_2Fe_{0.5}V_{0.5}$LDHs in 1 M KOH + c mM $NaVO_3$, respectively, scan rate of CV is 5 mV/s, EIS is tested at 0.6 $V_{Hg/HgO}$.

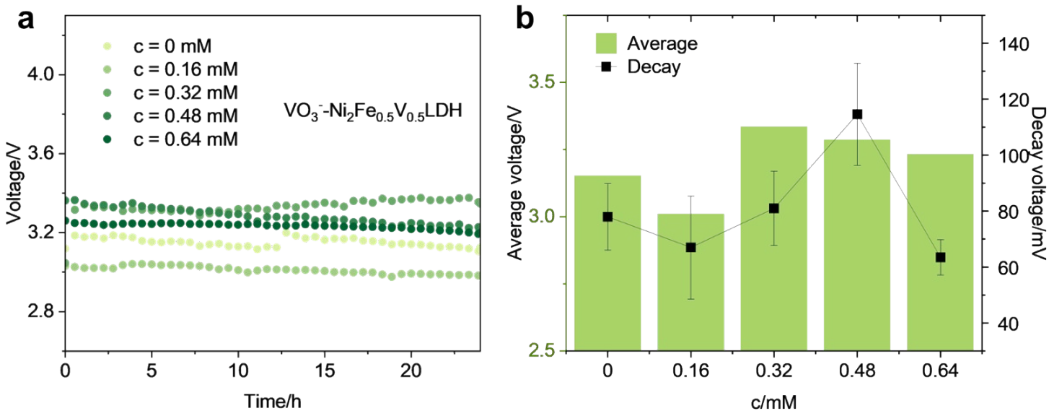

Figure S9. (a) Long-term stability curves of VO_3^--$Ni_2Fe_{0.5}V_{0.5}$LDHs in 1 M KOH + c mM $NaVO_3$ (400 mA/cm^2, 80℃, 24h) and (b) corresponding average voltage and decay voltage.

Table S2. Summary data of the activity and stability of eight NiFe-based LDHs with different electrolytes.

	Concentration of $NaVO_3$ in 1 M KOH/mM	η_{10mA} /V_{RHE}	Tafel slope /mV dec^{-1}	Average voltage/V	Decay voltage/mV
CO_3^{2-}-Ni_2Fe_1LDH	0	353	111.1	3.21628	53.46667
	0.16	347	103.1	3.22863	-21.43333
	0.32	342	100.8	3.14534	183.2
	0.48	340	92.7	3.47284	151.1
	0.64	340	92.3	3.12622	25.2
VO_3^--Ni_2Fe_1LDH	0	258	54.6	2.88	30.46667
	0.16	248	34.0	2.76035	-46.46667
	0.32	234	29.1	2.70305	-65.86667
	0.48	244	25.6	2.93823	-49.36667
	0.64	243	33.5	2.7748	-49.96667
$Ni_2Fe_{0.9}V_{0.1}$LDH	0	335	100.6	3.286	-34.1
$Ni_2Fe_{0.7}V_{0.3}$LDH	0	347	117.3	3.386	1.1
$Ni_2Fe_{0.5}V_{0.5}$LDH	0	306	113.7	3.173	-32.7
$Ni_2Fe_{0.3}V_{0.7}$LDH	0	331	151.0	3.399	-25.9
$Ni_2Fe_{0.1}V_{0.9}$LDH	0	329	151.7	3.228	22.9
VO_3^--$Ni_2Fe_{0.5}V_{0.5}$LDH	0	268	77.3	3.153	77.96667
	0.16	269	74.1	3.010	67
	0.32	265	73.0	3.335	81
	0.48	266	72.7	3.286	114.6
	0.64	264	71.0	3.233	63.46667

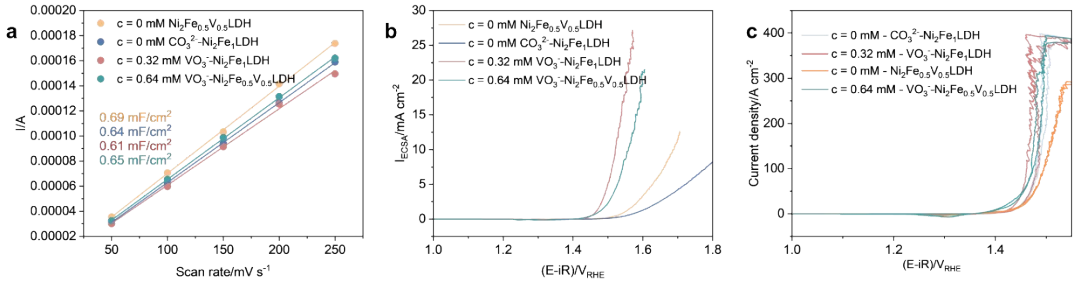

Figure S10. (a) The corresponding plots of current vs. scanning rate at voltage range from -0.1V to 0 $V_{Hg/HgO}$ and calculated C_{dl}, (b) LSV curves after ECSA normalization (I_{ECSA} = I/(C_{dl}/0.06)), (c) CV curves tested at 80°C.

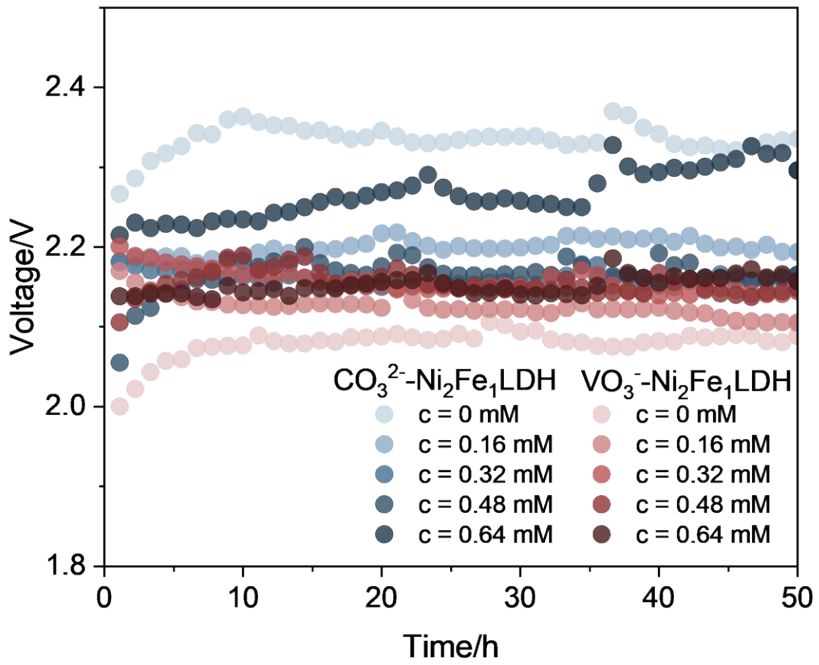

Figure S11. Long-term stability test of CO_3^{2-}-Ni_2Fe_1LDHs and VO_3^--NiFe LDHs in 1 M KOH + c mM $NaVO_3$. The substrate of catalyst is carbon paper.

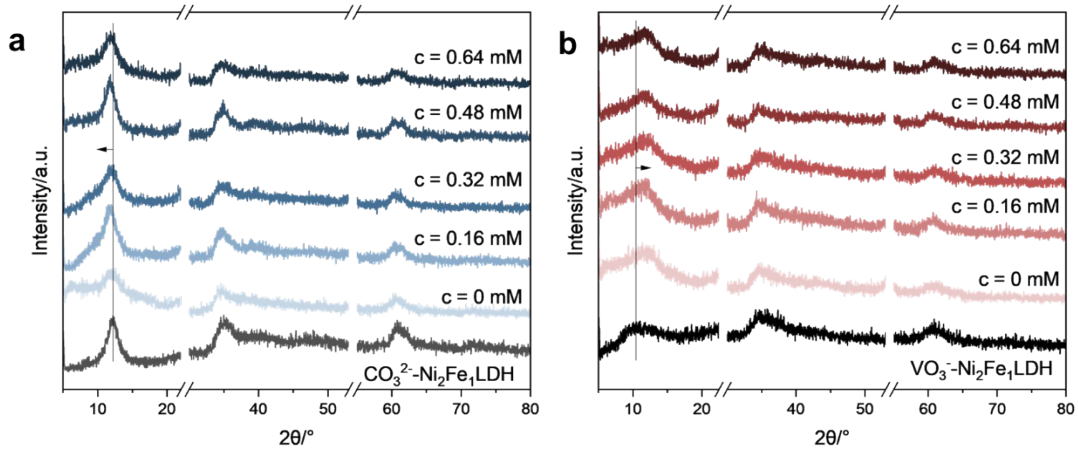

Figure S12. (a) and (b) the XRD patterns of CO_3^{2-}-Ni_2Fe_1LDHs and VO_3^--NiFe LDHs before (bottom line) and after stability test (50mA/cm^2, 50h, room temperature) in 1 M KOH + c mM $NaVO_3$.

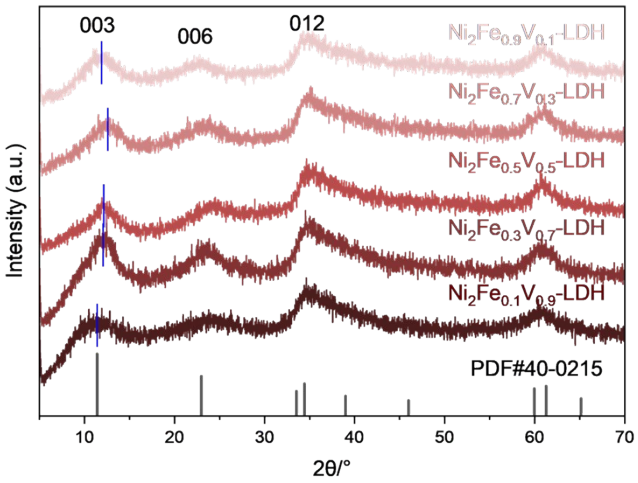

Figure S13. XRD pattern of $Ni_2Fe_xV_{(1-x)}$LDHs.

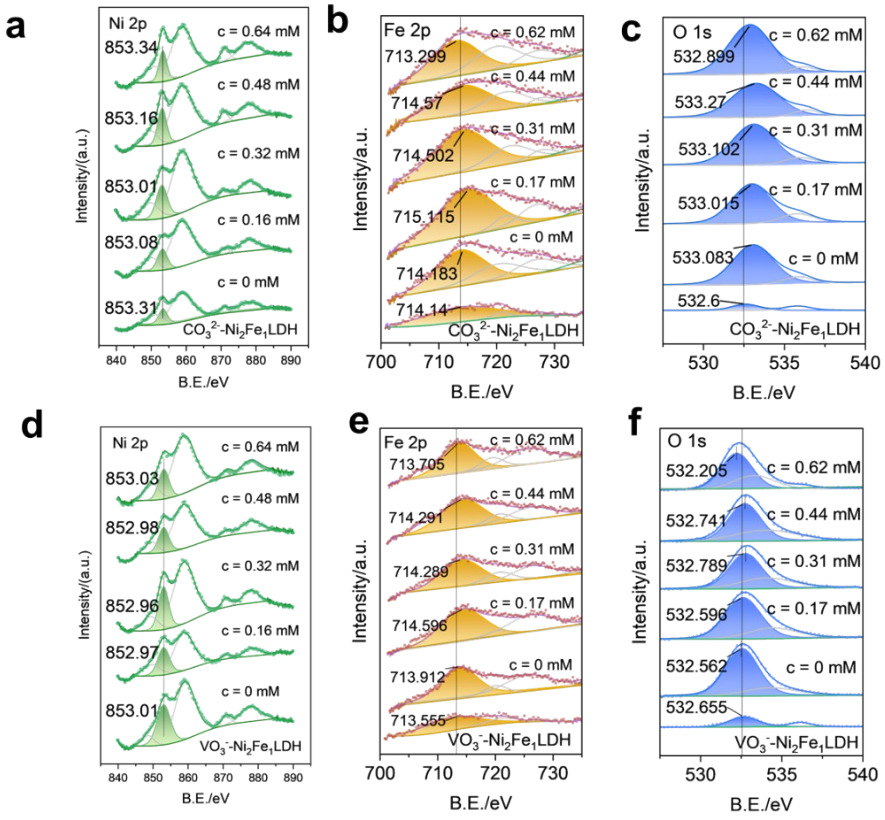

Figure S14. (a), (b), (c) XPS spectra for Ni 2p, Fe 2p, O 1s of CO_3^{2-}-Ni_2Fe_1LDHs before and after stability test (50mA/cm2, 50h, room temperature) in 1 M KOH + c mM $NaVO_3$, (d), (e), (f) XPS spectra for Ni 2p, Fe 2p, O 1s of VO_3^-- Ni_2Fe_1LDHs before and after stability test (50mA/cm2, 50h, room temperature) in 1 M KOH + c mM $NaVO_3$.

Table S3. Raman shifts of nickel oxides and hydroxides.[1]

	Raman Shift/cm^{-1}			
Compounds	**Ni-OH lattice mode**	**Ni-O lattice mode**	**2nd order lattice mode**	**O-H stretch**
α-$Ni(OH)_2$	460	495	935, 1075	3647
β-$Ni(OH)_2$	306-319	445-458	508-519	3581
γ-NiOOH	477		557	
β-NiOOH	492		557	

[1] a) B. C. Cornilsen, X. Y. Shan, P. L. Loyselle, *J. Power Sources.* **1990**, 29, 453.
b) W. Lai, L. H. Ge, H. M. Li, Y. L. Deng, B. Xu, B. Ouyang, E. Kan, *Int. J. Hydrogen Energy.* **2021**, 46, 26861.